

Induced long range dipole field enhanced antihydrogen formation in the $\bar{p} + Ps(n=2) \rightarrow e^- + \bar{H}(n \leq 2)$ reaction

Chi Yu Hu, David Caballero and Zoltán Papp

*Department of Physics and Astronomy, California State University, Long Beach, California
90840*

(November 20, 2018)

Abstract

We assume all interaction to be Coulombic and solve the modified Faddeev equation for energies between the $Ps(n=2)$ and $\bar{H}(n=3)$, which involve six and eight open channels. We find that 99% of the antihydrogen are formed in $\bar{H}(n=2)$. Just above the $Ps(n=2)$ threshold the S, P, and D partial waves contribute more than 4000 square Bohr radii near the maximum. Evidences indicate that the induced long range dipole potential from the degenerate $Ps(n=2)$ targets is responsible for such a large antihydrogen formation cross section.

PACS number(s): 36.10Dr, 34.90.+q

Due to the degeneracy of the excited hydrogen targets a long range dipole potential is induced in the field of the incoming charged particle. This potential is well known to be responsible for the formation of Feshbach resonances just below the $n \geq 2$ thresholds [1,2]. In the absence of relativistic effects and low lying open channels this attractive dipole potential can support an infinite set of bound states just below the threshold. Relativistic corrections remove the degeneracy and cut down the number of such states to only a few. The presence of low lying open channels embedding them in the continuum, they become resonant states and cause closely spaced oscillations in the cross section just below the threshold.

Gilitis and Damburg [2] pointed out that due to the Levinson theorem [3] similar oscillations exist just above the threshold. Our S-state cross sections in the energy gap between the $Ps(n=2)$ and $\bar{H}(n=3)$ thresholds indeed reveal such oscillations and the antihydrogen formation cross section is greatly enhanced in this region slightly above the $Ps(n=2)$ threshold. It is interesting to point out that the locations of the two Feshbach resonances below the $\bar{H}(n=3)$ threshold coincide almost exactly to the two minimums of the antihydrogen formation cross section curve. In addition, antihydrogen formation cross sections for P and D partial waves are calculated for a number of energies. It is shown that the total antihydrogen formation cross sections from S, P and D partial waves rise almost up to $1400\pi a_0^2$ near the maximum region.

The calculations are carried out using the modified Faddeev equations. The details of this method are given in Ref. [4]. We provide an outline below. The mass-scaled Jacobi vectors are defined as:

$$\mathbf{x}_\alpha = \tau_\alpha(\mathbf{r}_\beta - \mathbf{r}_\gamma), \quad \mathbf{y}_\alpha = \mu_\alpha \left(\mathbf{r}_\alpha - \frac{m_\beta \mathbf{r}_\beta + m_\gamma \mathbf{r}_\gamma}{m_\beta + m_\gamma} \right), \quad (1)$$

where $\tau_\alpha = \sqrt{2m_\beta m_\gamma / (m_\beta + m_\gamma)}$ and $\mu_\alpha = \sqrt{2m_\alpha(1 - m_\alpha/M)}$, $M = m_\alpha + m_\beta + m_\gamma$, and (α, β, γ) are cyclic permutations of $(1, 2, 3)$. The mass of the antiproton used is $m_1 = 1836.1527$, the mass of the electron and the positron are equal, $m_2 = m_3 = 1$ (the values are given in atomic units). The Jacobi vectors of different channels are related by the orthogonal transformation:

$$\begin{pmatrix} \mathbf{x}_\beta \\ \mathbf{y}_\beta \end{pmatrix} = \begin{pmatrix} C_{\beta\alpha} & S_{\beta\alpha} \\ -S_{\beta\alpha} & C_{\beta\alpha} \end{pmatrix} \begin{pmatrix} \mathbf{x}_\alpha \\ \mathbf{y}_\alpha \end{pmatrix}, \quad (2)$$

where

$$C_{\beta\alpha} = \left[\frac{m_\beta m_\alpha}{(M - m_\beta)(M - m_\alpha)} \right]^{1/2}, \quad (3)$$

$$S_{\beta\alpha} = (-1)^{\beta-\alpha} \text{sgn}(\alpha - \beta) (1 - C_{\beta\alpha}^2)^{1/2}. \quad (4)$$

In our particular case V_3 , the interaction between the \bar{p} and e^- , is a repulsive Coulomb potential which does not support two-body bound states. There are no asymptotic channels associated with this fragmentation. Consequently the total three-body wave function can be expressed in two components

$$\Psi = \psi_1(\mathbf{x}_1, \mathbf{y}_1) + \psi_2(\mathbf{x}_2, \mathbf{y}_2). \quad (5)$$

Asymptotically ψ_1 consists of an electron bound to the positron and a free antiproton, while ψ_2 , the rearrangement Faddeev component describes asymptotically an positron bound to the antiproton and a free electron.

We use the modified Faddeev equations:

$$(-\Delta_{x_\alpha} - \Delta_{y_\alpha} + V_\alpha + \bar{V}_\alpha - E)\psi_\alpha(\mathbf{x}_\alpha, \mathbf{y}_\alpha) = -V_\alpha^{(s)}\psi_\beta(\mathbf{x}_\beta, \mathbf{y}_\beta), \quad (6)$$

$\bar{V}_\alpha = V_3 + V_\beta^{(l)}$, $\alpha \neq \beta = 1, 2$, and V_1 and V_2 , the interactions between the (e^-, e^+) and (\bar{p}, e^+) pairs, respectively, are separated into short- and long-range terms

$$V_\alpha^{(s)} = V_\alpha(x_\alpha)\zeta_\alpha(x_\alpha, y_\alpha), \quad (7)$$

$$V_\alpha^{(l)} = V_\alpha(x_\alpha)(1 - \zeta_\alpha(x_\alpha, y_\alpha)). \quad (8)$$

The function $\zeta_\alpha(x_\alpha, y_\alpha)$ vanishes asymptotically within the three-body sector, where $x_\alpha \sim y_\alpha \rightarrow \infty$, and approaches one in the two-body cluster region, where $x_\alpha \ll y_\alpha \rightarrow \infty$. We use the following function having the required property:

$$\zeta(x, y) = 2 \{1 + \exp[(x/x_0)^\nu / (1 + y/y_0)]\}^{-1}, \quad (9)$$

where ν must be larger than 2 [4]. In principle, x_0 and y_0 are arbitrary, but they should be chosen to be consistent with the size of the scattering system for a rapid convergence.

In bipolar basis [5] the Faddeev component is given in the form

$$\Psi_\alpha(\mathbf{x}_\alpha, \mathbf{y}_\alpha) = \sum_{L=0}^{\infty} \sum_{M=-L}^L \sum_{\vec{l}+\vec{\lambda}=\vec{L}} \frac{\psi_{\alpha l \lambda}^L(x_\alpha, y_\alpha)}{x_\alpha y_\alpha} Y_{l \lambda}^{LM}(\hat{x}_\alpha, \hat{y}_\alpha) \quad (10)$$

where $Y_{l \lambda}^{LM}(\hat{x}_\alpha, \hat{y}_\alpha) = [Y_l^{m_l}(\hat{x}_\alpha) \times Y_\lambda^{m_\lambda}(\hat{y}_\alpha)]$, $\alpha = 1, 2$, and $\psi_{\alpha l \lambda}^L(x_\alpha, y_\alpha)$ is the partial component of the three-body wave function having total angular momentum L and relative angular momenta l and λ associated with coordinates \mathbf{x}_α and \mathbf{y}_α , respectively. Thus, for each L , the MFE [5] is further reduced to a set of two-dimensional partial differential equations:

$$\begin{aligned} (H_l^{(\alpha)} + V_\alpha - E)\psi_{\alpha l \lambda}^L(x_\alpha, y_\alpha) + \sum_{\vec{l}'+\vec{\lambda}'=\vec{L}} W_{l \lambda, l' \lambda'}^{(\alpha)L}(x_\alpha, y_\alpha) \psi_{\alpha l' \lambda'}^L(x_\alpha, y_\alpha) = \\ -V_\alpha^{(s)}(x_\alpha, y_\alpha) \sum_{\vec{l}'+\vec{\lambda}'=\vec{L}} \langle Y_{l \lambda}^{LM}(\hat{x}_\alpha, \hat{y}_\alpha) | \frac{\psi_{\beta l' \lambda'}^L(x_\beta, y_\beta)}{x_\beta y_\beta} Y_{l' \lambda'}^{LM}(\hat{x}_\beta, \hat{y}_\beta) \rangle, \end{aligned} \quad (11)$$

where

$$H_l^{(\alpha)} = -\partial_{x_\alpha}^2 - \partial_{y_\alpha}^2 + \frac{l(l+1)}{x_\alpha^2} + \frac{\lambda(\lambda+1)}{y_\alpha^2}, \quad (12)$$

$$W_{l \lambda, l' \lambda'}^{(\alpha)L}(x_\alpha, y_\alpha) = \langle Y_{l \lambda}^{LM}(\hat{x}_\alpha, \hat{y}_\alpha) | \bar{V}_\alpha | Y_{l' \lambda'}^{LM}(\hat{x}_\alpha, \hat{y}_\alpha) \rangle, \quad (13)$$

and $\beta \neq \alpha = 1, 2$.

The summation with respect to angular momentum channels is truncated in Eq. (11). When the proper cut-off parameters x_0 and y_0 in (9) is chosen the number of terms used for the S, P, and D partial waves ranges from 10 to 12 for the first Faddeev channel ($\bar{p} + Ps$), 8 to 10 for the second Faddeev channel ($e^- + \bar{H}$). The optimal choices of parameters satisfy the conditions $x_{\alpha_{max}} \approx 10x_0$; $y_{\alpha_{max}} \approx 10y_0$, $\alpha = 1, 2$, where $x_{\alpha_{max}}$, $y_{\alpha_{max}}$ are the respective cut-off distances which divide the asymptotic and interior regions. In the energy gap between $Ps(n=2)$ and $\bar{H}(n=3)$ we used 110a₀ and 75a₀ for $x_{\alpha_{max}}$, $\alpha = 1, 2$, and 450a₀ and 150a₀ for $y_{\alpha_{max}}$, respectively.

In the MFE approach the total three-body wave function $\psi^{(\sigma)}(x, y)$, for each open channel σ , is a vector having all $\psi_{\alpha\lambda}^L$ as its components. We further split the wave function into interior and asymptotic parts using the vector equation

$$\psi^{(\sigma)}(x, y) = F^{(\sigma)}(x, y) + f_{\sigma}^{(as)}(x, y) + \sum_{\sigma'=1}^{\sigma_{max}} \tilde{K}_{\sigma'\sigma} f_{as}^{(\sigma')}(x, y), \quad (14)$$

where $F^{(\sigma)}(x, y)|_{y_{\alpha} > y_{\alpha_{max}}} \equiv 0$, $f_{\sigma}^{(as)}(x, y)$ and $f_{as}^{(\sigma')}(x, y)$ are known incoming and outgoing asymptotic wave functions for the open channels σ when $y_{\alpha} > y_{\alpha_{max}}$ and they are equipped with spline continuity of values, first and second derivatives across the boundaries. They are otherwise identically zero in the interior regions. $\tilde{K}_{\sigma'\sigma}$ is related to the K-matrix by a kinematic factor [6].

The partial cross sections between the incoming channel i and the outgoing channel j with total angular momentum L is given by

$$\sigma_{ij} = \frac{\pi a_0^2}{k_i^2} (2L + 1) \left| \left(\frac{2K}{1 - iK} \right)_{ij} \right|^2, \quad (15)$$

where k_i is the momentum of the incoming channel.

Upon substitution of (14) into (11), we obtain the vector equation

$$(H - E)F^{(\sigma)}(x, y) = I_{\sigma} + \sum_{\sigma'=1}^{\sigma_{max}} \tilde{K}_{\sigma'\sigma} I^{(\sigma')}. \quad (16)$$

H is composed of two diagonal blocks of operators corresponding to the two Faddeev components on the left-hand side of (11) and two off-diagonal rectangular blocks involving the short-range potentials on the right-hand side of (11). I_{σ} , $I^{(\sigma')}$ are known inhomogeneous column vectors. Replace the unknown vector $F^{(\sigma)}(x, y)$ by $F^{(\sigma)}(x, y) = U_{\sigma}(x, y) + \sum_{\sigma'=1}^{\sigma_{max}} \tilde{K}_{\sigma',\sigma} U^{(\sigma')}$ in (16). We find the U 's satisfy the inhomogeneous equations

$$(H - E)U_{\sigma} = I_{\sigma} \quad (17)$$

$$(H - E)U^{(\sigma)} = I^{(\sigma)}, \quad \sigma = 1, \dots, \sigma_{max}. \quad (18)$$

The U 's are solved using fifth order Hermite polynomial spline expansion [5–7]. Matching the interior wave function $F^{(\sigma)}(x, y)$ with the known asymptotic wave functions at or near $y_{\alpha_{max}}$ we obtain highly over determined linear equations for the unknown $\tilde{K}_{\sigma'\sigma}$. Two independent methods are used for the solutions: (1) a standard least-square procedure and (2) projection on open channels. The details are given in [5,6].

The size of matrix equation used to solve (17,18) varies depending on the energy and the total angular momentum. They range from about 100000×100000 to 150000×150000 for results accurate at least 5%. The solutions are obtained using a solver in ScaLAPACK library on the massive parallel Blue Horizon IBM computer at the San Diego Supercomputer Center.

In the energy gap between $Ps(n=2)$ and $\bar{H}(n=3)$ there are six open channels for S partial wave. The elastic cross sections are plotted in Fig. 1, the horizontal axis plots energies in $Ps(n=2) + \bar{p}$ channel. The elastic cross section from $e^- + \bar{H}(1s)$ and $\bar{p} + Ps(1s)$ are relatively very small, they are not visible, that from $e^- + \bar{H}(2s)$ $e^- + \bar{H}(2p)$ are somewhat larger. They are plotted in Fig. 1, for comparison with the huge elastic cross sections from the channels $\bar{p} + Ps(2s)$ and $\bar{p} + Ps(2p)$. Due to the large induced dipole moment of the excited positronium, the Gilitis-Damburg oscillations are clearly seen in Fig. 1 below 0.003Ry, the energies are measured from the $Ps(n=2)$ threshold. The cross sections are rather monotonous between 0.003–0.008Ry. The structure below the $\bar{H}(n=3)$ threshold is due to the two S -state resonances located at 0.8835Ry 0.8875Ry measured from the $\bar{H}(1s)$ threshold, or 0.0090Ry and 0.0130Ry relative to $Ps(n=2)$ threshold. One notices that the oscillations of the two degenerate $2s$ and $2p$ channels are nearly 180° out of phase in the region of Feshbach resonances, although the effect is distorted by the statistical weight of $1/3$ on the $2p$ cross sections.

Fig. 2 presents the S -state antihydrogen formation cross sections in the same energy gap. The formation cross section are greatly enhanced in the oscillation region below 0.003Ry. The largest cross section calculated is $219\pi a_0^2$. The two minima below the $\bar{H}(n=3)$ threshold are located almost exactly at the location of the two Feshbach resonances [8,9].

Calculations of the P and D partial wave cross sections have been carried out for a number of energies in the oscillating region. There are 8 open channels and 64 partial cross sections, most of them will not be reported here. Table I presents all antihydrogen formation cross sections of S , P and D partial waves at four energies. There are 9 antihydrogen formation partial cross sections for S -wave and 16 such partial cross sections for P and D waves, respectively. We group them into three partial sums, $\sigma_L^{(1)}$, $\sigma_L^{(2)}$ and $\sigma_L^{(3)}$, where L is the angular momentum (S, P, D). $\sigma_L^{(1)}$ is the sum of all partial cross sections with antihydrogen formed in $1s$ state. $\sigma_L^{(2)}$ is the sum of all partial cross sections having antihydrogen formed in $2s$ and $2p$ states but originated from $Ps(1s)$ target. $\sigma_L^{(3)}$ is the sum of all partial cross sections with antihydrogen formed in $2s$ and $2p$ states but originated from excited Ps targets.

Our calculations highlight three important points:

1. The P and D partial waves follow the same tendency of strong oscillations near $Ps(n=2)$ threshold similarly to that of S -partial wave. Table I shows as σ_S increases towards the $Ps(n=2)$ threshold, so do σ_P and σ_D . Seaton [1] pointed out that the strength of the dipole potential from $n=2$ target can support Feshbach resonances for all partial waves with $L \leq 2$.
2. Since the cross section depend on the kinematic factor $1/k_i^2$ in (15), where k_i is the momentum of the incoming channel, the oscillations are amplified near the lower threshold $Ps(n=2)$, and hence the antihydrogen formation cross sections are also greatly enhanced. On the other hand, the Feshbach resonances just below the upper $\bar{H}(n=3)$

threshold have negligible contribution to the antihydrogen formation cross sections. In fact, Fig. 2 shows two minima in antihydrogen formation cross section located at 0.8835Ry and 0.8875Ry above $\bar{H}(1s)$ threshold, respectively. Archer and Parker [8] found one S -state resonance at -0.11492 Ry below breakup, or 0.88454Ry above $\bar{H}(1s)$. Ho and Green [9] found two S -state resonances at -0.11606 Ry and -0.11206 Ry below breakup, or 0.88340Ry and 0.88740Ry above $\bar{H}(1s)$. We used the threshold energy -0.99946 Ry for $\bar{H}(1s)$, due to finite \bar{p} mass, to calculate all resonance positions. In comparison, our novel method to determine Feshbach resonance position seems to have at least three to four digits of accuracy!

3. Not surprisingly, the long range polarization potential, mainly the dipole potential, couples strongly only amongst the excited $2s$ and $2p$ states which lie just below the targets $Ps(n=2)$. The ground states $Ps(1s)$ and $\bar{H}(1s)$ contribute less than 2% of the antihydrogen formation cross section, and even less of them are formed in $\bar{H}(1s)$. As a result, near 99% of the antihydrogen are formed in $2s$ and $2p$ states with $Ps(n=2)$ targets.

Archer and Parker [8] solved the Schrödinger equation using a form of hyperspherical coordinates. They calculated S -state partial cross sections up to $H(n=4)$ threshold. However, they purposely avoided the long range polarization potentials by projecting out only those with ground states targets and using cut-off hyperradius of $\rho = 120.0a_0$. We used cut-off coordinates that are equivalent to $\rho \approx 470a_0$. Our corresponding partial cross sections in the energy-gap between $Ps(n=2)$ and $\bar{H}(n=3)$ are generally 25% lower. The complete coupling of all six open channels in our calculation may be responsible for the differences.

Igarashi et. al. [10] made hyperspherical coupled-channel calculations for antihydrogen formation in a broad range of energies in $\bar{p} + Ps$ scattering including partial waves up to angular momentum $L = 12$ and included cross section from Born approximations for $L \geq 13$. Unfortunately there is only one of their energy points fell within the gap between $Ps(n=2)$ and $\bar{H}(n=3)$ thresholds. This point is located at ~ 0.002 Ry, its total formation cross section is approximately $640\pi a_0^2$, where our value at this point is approximately $396\pi a_0^2$ from three partial waves. This means that, at least at this energy, the lowest three partial waves contribute about 62% of the total formation cross section. Fig. 2 and Table I show that this energy point is not in the region of optimal antihydrogen formation. Our largest calculated antihydrogen formation cross section is $1397\pi a_0^2$ from the lowest three partial waves. The energy at this point is 0.000494Ry. Table I shows that at this energy $\sigma_D/\sigma_S = 3.15$. This is less than the factor $2L+1$ in (15). But it is expected that higher partial waves contribute much less effectively at such low energy. The long range dipole potential from $Ps(n=2)$ targets is expected to cause oscillations for all partial waves with $L \leq 2$. We expect a much more drastic drop in σ_L/σ_S for $L \geq 3$. Works are in progress to calculate contributions from $L \geq 3$.

ACKNOWLEDGMENTS

This work has been supported by the NSF Grant No.Phys-0088936. We also acknowledge the generous allocation of computer time at the NPACI, formerly San Diego Supercomputing Center.

REFERENCES

- [1] M. J. Seaton, Proc. Phys. Soc. **77**, 174 (1961).
- [2] M. Gailitis and R. Damburg, Soviet Phys. JETP **17**, 1107 (1963).
- [3] N. Levinson, Kgl. Danske Videnskab. Selskab, Mat.-fys. Medd., **25**, 9 (1949).
- [4] S. P. Merkuriev, Ann. Phys. (N.Y.) **130**, 395, (1980); L. D. Faddeev and S. P. Merkuriev, *Quantum Scattering Theory for Several Particle Systems*, (Kluwer, Dordrecht, 1993), Chap. 7.
- [5] C.-Y. Hu, J. Phys. B: At. Mol. Opt. Phys. **32**, 3077 (1999).
- [6] A. A. Kvitsinsky and C.-Y. Hu, J. Phys. B: At. Mol. Opt. Phys. **29**, 2059 (1996).
- [7] C.-Y. Hu and A. A. Kvitsinsky, Hyperfine Interactions, **82**, 59 (1993).
- [8] B. J. Archer and G. A. Parker, Phys. Rev. A **44**, 1303 (1990).
- [9] Y. K. Ho and C. H. Greene, Phys. Rev. A **35**, 3169 (1987).
- [10] A. Igarashi, N. Toshima and T. Shirai, J. Phys. B: At. Mol. Opt. Phys. **27**, L497 (1994).

TABLES

TABLE I. Antihydrogen formation cross sections and partial cross sections for processes $\bar{p} + Ps(n \leq 2) \rightarrow e^- + \bar{H}(1s)$, $\bar{p} + Ps(n = 1) \rightarrow e^- + \bar{H}(n = 2)$ and $\bar{p} + Ps(n = 2) \rightarrow e^- + \bar{H}(n = 2)$. The corresponding partial cross sections are denoted by $\sigma_L^{(1)}$, $\sigma_L^{(2)}$ and $\sigma_L^{(3)}$, respectively, and $L = S, P, D$. The energy values (in Ry) are measured from the $\bar{H}(1s)$ threshold and the cross sections are given in πa_0^2 units. $\sigma_L = \sum_i \sigma_L^{(i)}$ is the total formation cross section for the partial wave L .

	Energy			
	0.8749	0.8755	0.877	0.8799
$\sigma_S^{(1)}$	0.282	0.097	0.047	0.030
$\sigma_S^{(2)}$	0.125	0.116	0.112	0.107
$\sigma_S^{(3)}$	218.84	76.701	32.481	17.201
σ_S	219.25	76.914	32.640	17.338
$\sigma_P^{(1)}$	3.373	1.783	1.130	0.886
$\sigma_P^{(2)}$	1.041	1.042	1.015	1.040
$\sigma_P^{(3)}$	482.65	226.62	101.91	50.73
σ_P	487.06	229.45	104.06	52.66
$\sigma_D^{(1)}$	7.841	4.214	2.668	2.087
$\sigma_D^{(2)}$	1.076	1.068	1.047	1.099
$\sigma_D^{(3)}$	682.02	312.94	162.91	76.174
σ_D	690.94	318.22	166.63	79.36
$\sum_{L=S,P,D} \sigma_L^{(1)}$	11.496	6.094	3.845	3.003
$\sum_{L=S,P,D} \sigma_L^{(2)}$	2.242	2.226	2.174	2.246
$\sum_{L=S,P,D} \sigma_L^{(3)}$	1383.51	616.26	297.31	144.11
$\sum_{L=S,P,D} \sigma_L$	1397.25	624.58	303.33	149.36

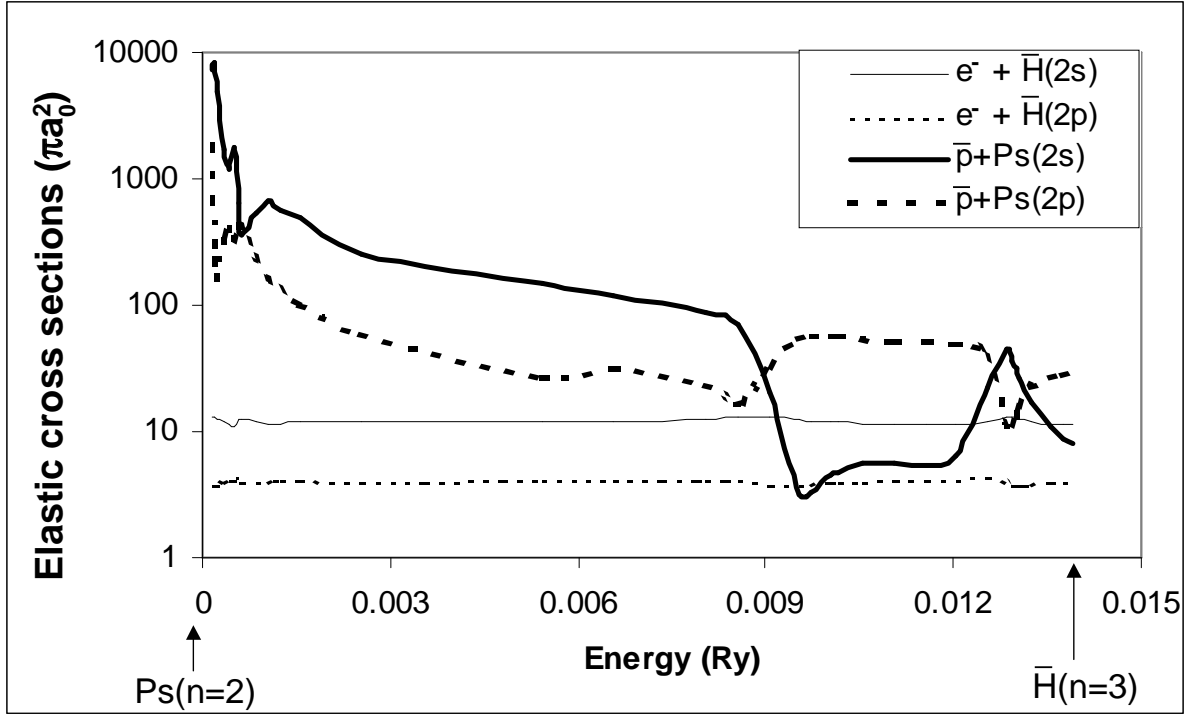


FIG. 1. Elastic cross sections of the processes $e^- + \bar{H}(2s)$, $e^- + \bar{H}(2p)$, $\bar{p} + Ps(2s)$ and $\bar{p} + Ps(2p)$. All energies are measured from the $Ps(n = 2)$ threshold. The $\bar{H}(n = 3)$ threshold is located at $0.01395 Ry$.

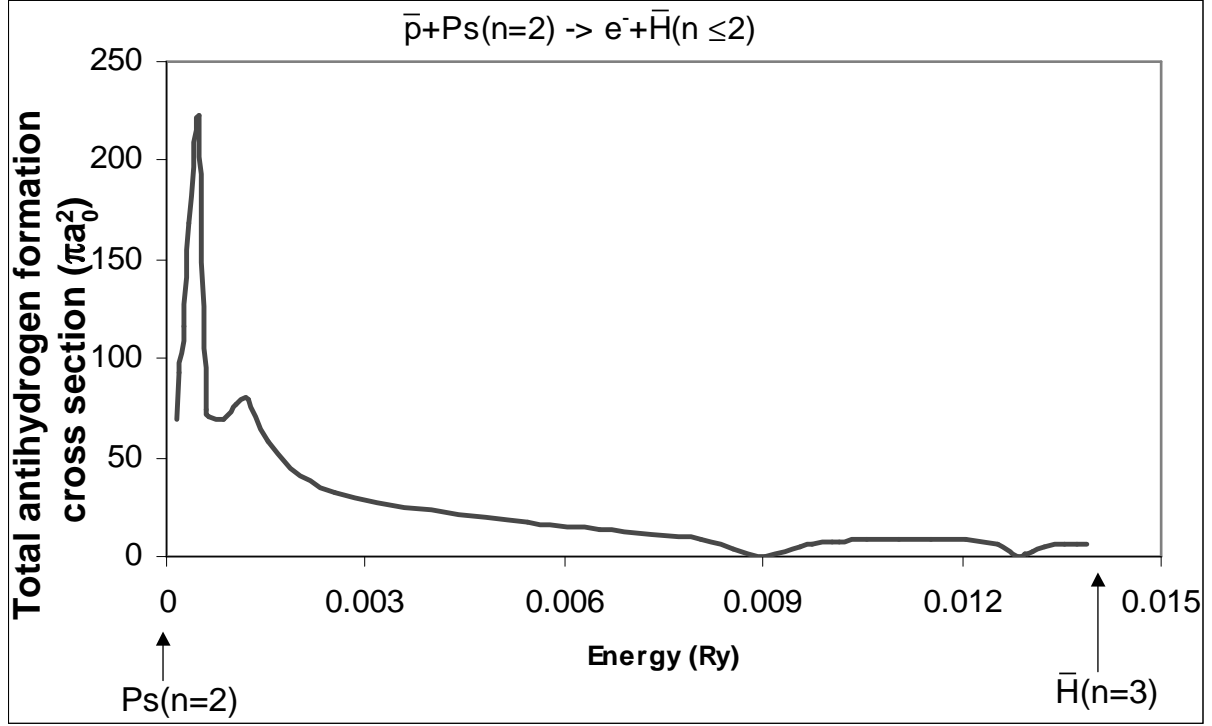


FIG. 2. Antihydrogen formation cross sections from all the processes $\bar{p} + Ps(n \leq 2) \rightarrow e^- + \bar{H}(n \leq 2)$. The energies are measured from the $Ps(n=2)$ threshold.